

# PHYSICAL REVIEW LETTERS

---

---

VOLUME 53

17 SEPTEMBER 1984

NUMBER 12

---

---

## Building Blocks of Percolation Clusters: Volatile Fractals

Hans J. Herrmann and H. Eugene Stanley

*Service de Physique Theorique, Centre d'Etudes Nucléaires de Saclay, F-91191 Gif-sur-Yvette Cedex, France, and  
Center for Polymer Studies and Department of Physics, Boston University, Boston, Massachusetts 02215*

(Received 26 June 1984)

We solve for the internal structure of  $d$ -dimensional percolation clusters. We find that if we randomly choose two points, then the backbone connecting these two points can be described as a randomly constructed "necklace" whose building blocks are  $s$ -site volatile fractals (they are not stable under a length scale change). We find the blob-size distribution function and calculate the relevant parameters numerically, thereby obtaining the first accurate estimates for the fractal dimension of the backbone in  $d = 2, 3$ .

PACS numbers: 05.40.+j, 05.70.Jk

What is the internal structure or "texture" of a percolation cluster? This important question has eluded definitive answers despite much recent interest in the use of percolation to describe a vast number of physical phenomena ranging from aggregation of proteins to galaxy structure. Some answer is urgently needed, as recent models for the elasticity of gels<sup>1,2</sup> (and the conductivity of random mixtures<sup>3</sup>) depend crucially on cluster structure since they both address the question of the percolation backbone: the set of bonds that carry stress (or current) when one singles out two points of a large cluster.

Three pictures of cluster structure have been proposed. In model 1, the cluster just above the percolation threshold  $p_c$  is imagined to resemble a large fisherman's net: It is composed of singly connected links and nodes where the links join one another.<sup>4</sup> The correlation length is a rough measure of the characteristic size of fish that will be caught. Model 2 is the opposite extreme of the nodes and links picture: It replaces the cluster by a Sierpinski gasket and so has no singly connected links but does have multiply connected "blobs" of all length scales.<sup>5</sup> Model 3, the links-nodes-blobs model, is a hybrid model in which multiply connected blobs are strung along the links of model 1.<sup>6,7</sup>

From recent applications of percolation to systems in nature, it is becoming increasingly clear that model 3 has many advantages. However, despite this fact, nothing<sup>8</sup> is known about the blobs: We know that they "exist," but we cannot make any quantitative or even qualitative statements about their characteristics. Here we attempt to correct this deplorable situation. Our initial purpose was to address the problem of obtaining the complete statistical distribution of the blobs. In so doing, we discovered that the blobs are a case of volatile fractals: At different length scales the blobs *themselves* change identity. Moreover, we find that the entire backbone is identical to what one would find if a drunk assembled a necklace of pearls, where the pearls are of all different sizes chosen according to the blob-size distribution function [Eq. (1) below].

We begin by considering the incipient infinite cluster<sup>6,7</sup>—operationally, the largest cluster in a large box of side  $L$  when  $p = p_c$ . Choose two points  $P$  and  $Q$  separated by a distance comparable to the box size  $L$ . If  $P$  and  $Q$  belong to the same cluster, then the backbone is the set of sites through which current would flow if the sites are regarded as metallic checkers that just touch their neighbors. Sites which if removed would result in a cessation of current are termed red<sup>6,7</sup>; red sites are also called

blobs of size one. All remaining backbone sites are members of blobs of size larger than one, and the backbone may be viewed as a topologically linear “necklace” of strings of blobs of *all* possible sizes and shapes [Fig. 1(a)]. Note that the blobs are volatile fractals: When  $L$  is increased smaller blobs can become part of larger blobs [Fig. 1(b)].

To describe these volatile fractals, we introduce the blob-size distribution function  $n_s(L)$  which gives the number of blobs of size  $s$  in a box of edge  $L$ . We propose the scaling *Ansatz*

$$n_s(L) \sim s^{-\tau} f(s/L^{d_f^{\text{BB}}}). \quad (1a)$$

Here

$$\tau - 1 = d/d_f^{\text{BB}}, \quad (1b)$$

where  $d_f^{\text{BB}}$  is the fractal dimension of the backbone. Now we know that  $n_s(L) \rightarrow 0$  when  $L \rightarrow \infty$  because the small blobs become big blobs when the system is viewed under a larger length scale  $L$ . Hence we expect that the scaling function  $f(x)$  ap-

proaches zero when  $L \rightarrow \infty$  for fixed  $s$ :  $f(x) \sim x^y$  with  $y > 0$ .

To study the blobs at a given box size  $L$ , we use a scaling function  $\tilde{f}(x) \equiv x^{-y} f(x)$  in (1), and obtain

$$n_s(L) \sim L^{d_r - d} s^{-\tilde{\tau}} \tilde{f}(s/L^{d_f^{\text{BB}}}). \quad (2a)$$

Here

$$\tilde{\tau} - 1 = d_r/d_f^{\text{BB}}, \quad (2b)$$

where  $d_r$  is the exponent describing how the number of blobs increases with  $L$ . The exponent  $y = (d - d_r)/d_f^{\text{BB}}$ , a ratio of dimensions, is universal with respect to the “kinetics”; i.e., it does not change even for a nonanalytic change of the “time” variable ( $p - p_c$ ). These kinetic aspects are intriguing because of the formal similarity of (2) with cluster-size distribution functions in aggregation phenomena,<sup>9</sup> where this observation should also be useful.

Note from (2) that the total density of blobs,  $\sum_s n_s$ , usually a background term, should decrease as  $L^{d_r - d}$ . Because of self-similarity, the number of red sites (blobs of size unity) is proportional to the total number of blobs; hence  $d_r$  is also the fractal dimension of the red sites. Since  $d_r = y_T$ , the thermal scaling field,<sup>8</sup> it follows that the scaling field due to  $p - p_c$  comes in *at*  $p_c$  in the finite-size scaling of blobs, but not of clusters [cf. Eqs. (1) and (2)].

Next we test the scaling relations (1) and (2) numerically, and thereby extract from the calculations extremely accurate values of the relevant fractal dimensions. Since it has not been possible in the past to measure the size of the blobs of the backbone, we first describe our method in some detail. *Step 1*: Determine the cluster backbone using the “burning” method<sup>10</sup>; this requires choosing two points  $P$  and  $Q$  of the largest cluster in a box of edge  $L$ , and we choose these two points to be those closest to diagonally opposite corners of the box. *Step 2*: Identify the set of all “shortest” paths from  $P$  to  $Q$ ; the elastic backbone is specially indexed with increasing numbers for measuring the chemical distance from  $P$ . *Step 3*: Starting from  $P$ , go one by one through the sites of the elastic backbone. From each site, we burn until no more sites can be burned, using the rule that a site once burned can never be burned again (like trees in a forest); a burning site burns all neighbors except for the case when the site and its neighbor are indexed and the index of the neighbor is larger than that of the burning site. Thus for each site of the elastic backbone, a certain “mass” is burned. These masses are summed until we reach a site of the elastic backbone that is not able to burn, but has itself not been burned. This site finishes a blob. Then the mass of the blob is registered and a new mass count

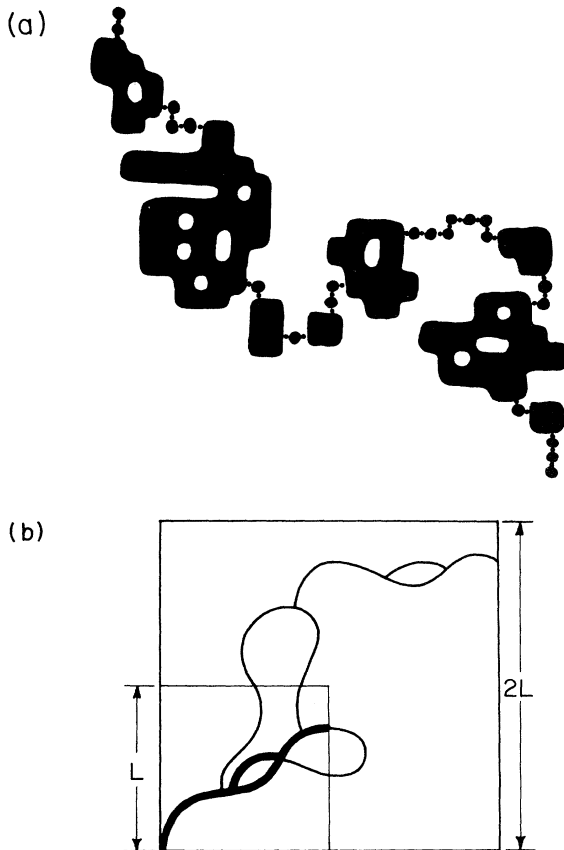


FIG. 1. (a) Actual simulation of a backbone in site percolation on a square lattice; the decomposition into blobs of all sizes from 1 to  $\infty$  is apparent. (b) Schematic illustration of how small blobs become part of larger blobs when the box size  $L$  is increased.

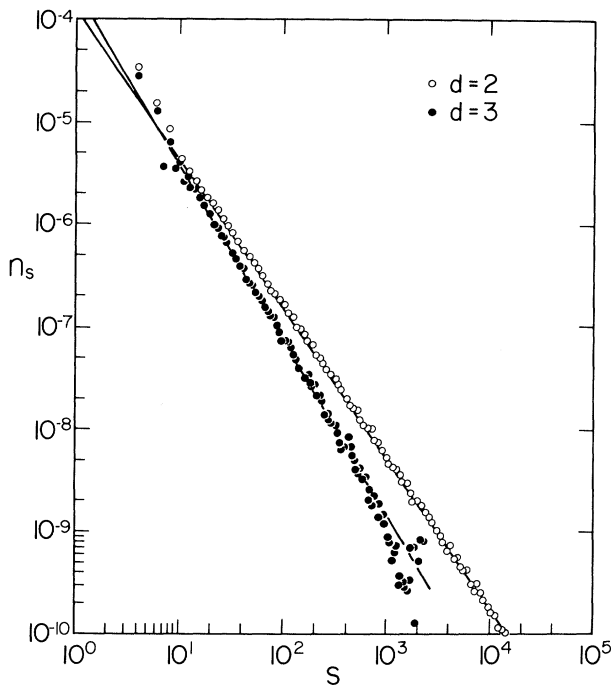
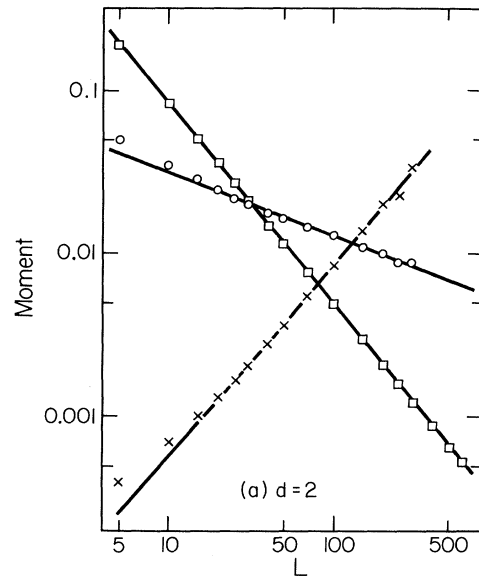


FIG. 2. Blob-size distribution function for  $d=2, 3$  for  $L=600$  ( $d=2$ ) and  $L=60$  ( $d=3$ ).

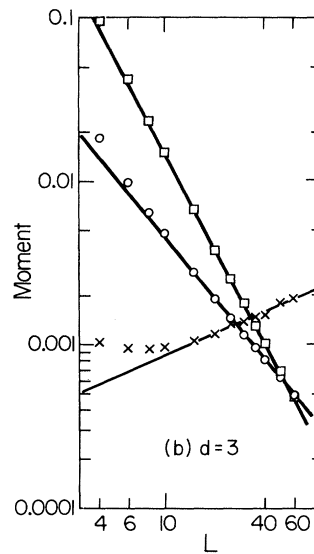
starts for the next blob.

We thereby calculated the *complete* statistical distribution  $n_s(L)$  for a sequence of seventeen  $L$  values up to  $L=600$  for  $d=2$ , and for twelve  $L$  values up to  $L=60$  for  $d=3$ . The linearity over five decades of Fig. 2 confirms the validity of the scaling *Ansatz*; from the slopes, we find  $\tilde{\tau}=1.45 \pm 0.05$  ( $d=2$ ) and  $1.67 \pm 0.05$  ( $d=3$ ). That  $\tilde{\tau} < 2$  is at first sight surprising, because usually  $\tau < 2$  cannot hold for size distribution functions as a consequence of mass conservation. However, the scaling relation (2) explains why  $\tau < 2$ , and to test (2) we show (Fig. 3) the moments  $\sum_s s^k n_s$  in a log-log plot against system size  $L$ . From the  $k=0$  plot we find slopes  $-1.24 \pm 0.02$  ( $d=2$ ) and  $-1.89 \pm 0.02$  ( $d=3$ ) which agree with the predictions  $d_r - d = -\frac{5}{4}$  ( $d=2$ ) and  $-1.89$  ( $d=3$ ).<sup>11</sup> This agreement serves to provide striking confirmation of the relation (2). Hence we can substitute the values of  $\tilde{\tau}$  and of  $d_r = \gamma_\tau$  in (2b) to obtain estimates for  $d_f^{BB}$ :  $1.67 \pm 0.17$  ( $d=2$ ) and  $1.68 \pm 0.14$  ( $d=3$ ), which are consistent with independent estimates.<sup>12</sup>

The error bars can be reduced by an order of magnitude by taking advantage of the scaling relation (2). The first and second moments have exponents  $(2-\tau)d_f^{BB}$  and  $(3-\tau)d_f^{BB}$ , respectively, which we find to be  $-0.37 \pm 0.01$  and  $1.19 \pm 0.03$  ( $d=2$ ) and  $-1.21 \pm 0.03$  and  $0.47 \pm 0.06$  ( $d=3$ ).



(a)  $d=2$



(b)  $d=3$

FIG. 3. The moments  $\sum_s s^k n_s$  of the blob-size distribution function  $n_s$  for  $k=0$  (squares),  $k=1$  (circles), and  $k=2$  (crosses).

From these numbers, we find  $\tau=2.237 \pm 0.015$  ( $d=2$ ), an accuracy of *better than 1%*, and  $\tau=2.72 \pm 0.05$  ( $d=3$ ). Using these extremely accurate estimates of  $\tau$ , we can use the relation  $d_f^{BB} = d/(\tau-1)$  to obtain  $d_f^{BB}=1.62 \pm 0.02$  ( $d=2$ ) and  $1.74 \pm 0.04$  ( $d=3$ ), which are by far the most accurate estimates of the backbone fractal dimension published.<sup>12</sup>

The above remarks concern the *blob-size distribution*. Can we also predict the *blob arrangement*?

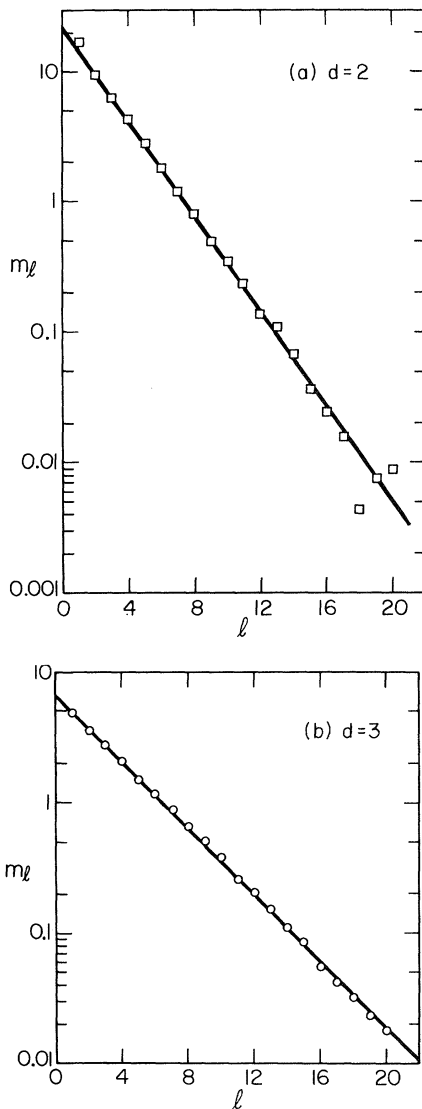


FIG. 4. Semilog plot showing the frequency  $m_l$  that one finds a string of red sites of length  $l$ , for  $d=2, 3$ .

Topologically speaking, the backbone is a necklace of blobs of all sizes. Consider the frequency of occurrence of a sequence or "string" of  $l$  successive red sites. If the red sites are chosen *at random* from the distribution law (1), then the probability of a string of  $l$  sites is given by  $m \sim \pi^l \sim \exp(-l \log \pi)$ , where  $\pi = n_1 / \sum_s n_s$  is the probability that a blob *selected at random* has size one. Hence the slope of Fig. 4 should be given by  $\log \pi$ . From our cluster-size data we predict that  $\pi = 0.69 \pm 0.05$  ( $d=2$ ) and  $0.77 \pm 0.01$  ( $d=3$ ), while from Fig. 4  $\pi = 0.68 \pm 0.01$  ( $d=2$ ) and  $0.76 \pm 0.01$  ( $d=3$ ). This striking agreement confirms the quantitative

picture that the backbone is a "pearl" necklace assembled from a distribution of pearl sizes, chosen according to the distribution law (1), and assembled in completely random order.

In summary, we have proposed a scaling law for the blob-size distribution function of the percolation backbone. We have confirmed this distribution for a sequence of box sizes up to  $L=600$  ( $d=2$ ) and  $L=60$  ( $d=3$ ) and found that the blobs are volatile fractals: Their identity changes with box size, as the smaller blobs become "eaten up" by larger blobs when  $L$  increases. We have used this distribution to calculate the probability of finding a string of red sites of length  $l$ , and have tested this prediction numerically. While a linear polymer is a pearl necklace with identical pearls, a percolation backbone is a necklace whose pearls have a distribution of sizes which are chosen from the distribution law (1) and which are otherwise selected completely at random.

We wish to thank A. Coniglio, D. C. Hong, and D. Stauffer for stimulating discussions, and the U. S. Office of Naval Research and National Science Foundation for financial support.

<sup>1</sup>S. Feng and P. N. Sen, Phys. Rev. Lett. **52**, 216 (1984).

<sup>2</sup>Y. Kantor and I. Webman, Phys. Rev. Lett. **52**, 1891 (1984).

<sup>3</sup>R. Zallen, *The Physics of Amorphous Solids* (Wiley, New York, 1983).

<sup>4</sup>A. Skal and B. I. Shklovskii, Fiz. Tekh. Poluprovodn. **8**, 1586 (1974) [Sov. Phys. Semicond. **8**, 1029 (1975)]; P. G. de Gennes, J. Phys. (Paris) Lett. **37**, L1 (1976).

<sup>5</sup>Y. Gefen, A. Aharony, B. B. Mandelbrot, and S. Kirkpatrick, Phys. Rev. Lett. **47**, 1771 (1981).

<sup>6</sup>H. E. Stanley, J. Phys. A **10**, L211 (1977).

<sup>7</sup>A. Coniglio, Phys. Rev. Lett. **46**, 250 (1981), and J. Phys. A **15**, 3829 (1982); see also R. Pike and H. E. Stanley, J. Phys. A **14**, L169 (1981). A recent review is given by H. E. Stanley and A. Coniglio, Ann. Isr. Phys. Soc. **5**, 101 (1983).

<sup>8</sup>One *rigorous* result (Ref. 7) concerns the fashion in which the mass of the "red sites" scales with the length scale  $L$  on which they are examined,  $(\text{Mass})_{\text{red}} \sim L^{d_r}$ :  $d_r = y_T$ .

<sup>9</sup>T. Vicsek and F. Family, Phys. Rev. Lett. **52**, 1669 (1984); M. Kolb, to be published.

<sup>10</sup>H. J. Herrmann, D. Hong, and H. E. Stanley, J. Phys. A **17**, L261 (1984).

<sup>11</sup>We use  $d_r = y_T$  and  $y_T = \frac{3}{4}$  ( $d=2$ ) and the estimate  $y_T^{-1} = 0.89 \pm 0.01$  ( $d=3$ ) [See D. W. Heermann and D. Stauffer, Z. Phys. B **44**, 339 (1981).]

<sup>12</sup>See Table I of D. C. Hong and H. E. Stanley, J. Phys. A **16**, L475 (1983).